氏　　名	LE PHUONG SON		
学位の種類	博士(マテリアルサイエンス)		
学位記番号	博材第 355 号		
学位授与年月日	平成 26 年 9 月 24 日		
論文題目	Low-frequency noise of narrow-and wide-gap Ⅲ - Ⅴ compound semiconductor devices.（ナローギャップ・ワイドギャップⅢ-Ⅴ族化合物半導体デバイスにおける低周波雑音）		
論文審査委員	主査	鈴木　寿一	北陸先端科学技術大学院大学　教授
		下田　達也	同　教授
		富取　正彦	同　教授
		山田　省二	同　教授
		前澤　宏一	富山大学　教授

Low-frequency noise in narrow- and wide-gap III-V compound semiconductor devices

Suzuki Laboratory s1140211 LE Phuong Son

1 Introduction

III-V compound semiconductors, which have many advantages over silicon, are important materials for electronic and optical devices. For example, InAs, which has a narrow energy gap E_g and a very high electron mobility μ, is a potential material for high-speed device applications. In contrast to InAs, GaN, which has a wide E_g and a moderate μ, is a promising material for high-power device applications. Although III-V compound semiconductor devices have been studied for a long time [1–3], their low-frequency noise (LFN) characterization still remains many issues.

In this work, we fabricated two-terminal (2T) devices from InAs films obtained by separation-bonding method on low-k flexible substrates (FS) (InAs/FS) [4, 5] or by direct growth on GaAs(001) (InAs/GaAs). In addition, from $Al_{0.27}Ga_{0.73}N$/GaN heterostructures, we fabricated GaN devices, ungated 2T devices as well as heterojunction field-effect transistors (HFETs), with Schottky structures and metal-insulator-semiconductor (MIS) structures in which an AlN insulator was sputtering-deposited on the AlGaN [6, 7]. Before the AlN deposition, two types of the AlGaN surface treatment were used with and without a cleaning by Semicoclean (an ammonium-based solution, ABS). Using these devices, LFN in InAs and GaN devices were investigated by using a measurement system with configurations shown in Fig. 1(a) for 2T devices and (b) for HFETs.

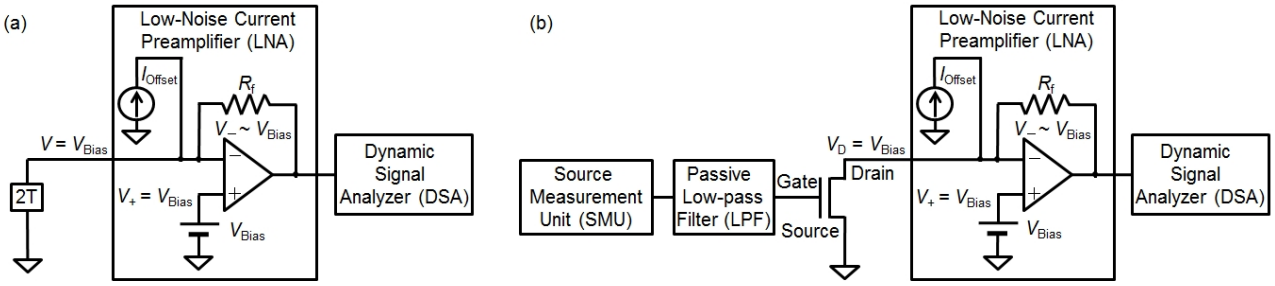

Figure 1: Low-frequency noise measurement system for (a) 2T devices and (b) HFETs.

2 Low-frequency noise in InAs films bonded on low-k flexible substrates or grown on GaAs(001)

Figures 2(a) and (b) show the mobility μ as functions of the InAs thickness d and the sheet electron concentration n_s, respectively. The LFN in InAs devices shown in Figs. 2(c) and (d) exhibits that the current noise power spectrum density S_I satisfies $S_I/I^2 \simeq K/f$ with current I and frequency f, where K is a constant.

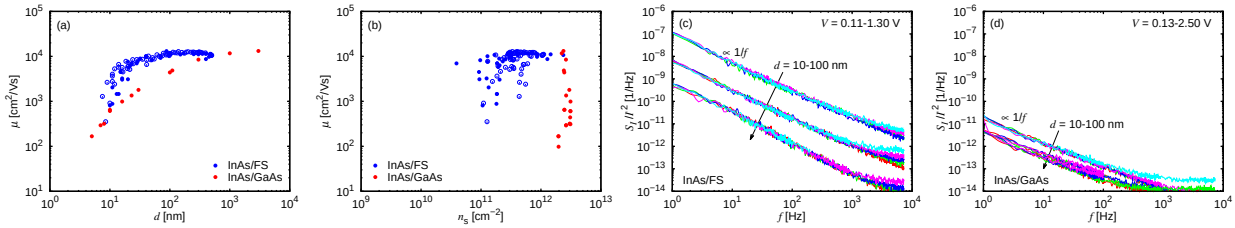

Figure 2: The mobility μ as functions of (a) the InAs thickness d and (b) the sheet electron concentration n_s. S_I/I^2 as functions of f for (c) InAs/FS and (d) InAs/GaAs with $d \simeq 10,\ 30,\ 100$ nm.

Figures 3(a) and (b) show $S_I f$ as functions of I to determine K. Since the device resistance is the sum of the contact resistance $R_c = r_c/W$ and the InAs channel resistance $R_{ch} = r_s L/W$ with the contact resistivity r_c, the sheet resistance r_s, the channel length L, and the device width W, the factor K is given by

$$KW = \frac{(K_c W/2) + (\alpha/n_s)(r_s/2r_c)^2 L}{[1 + (r_s/2r_c)L]^2}, \tag{1}$$

where K_c is the factor for one contact, α and n_s are the Hooge parameter and the sheet electron concentration of the InAs channel, respectively. Figures 3(c) and (d) show KW as functions of L with fitting lines using Eq. (1), exhibiting $K \propto 1/LW$, which indicates a negligible contribution of the contacts. The LFN is hence dominated by the channel, and the Hooge parameter can be calculated by $\alpha = KN = Kn_sLW$, where N is the electron number in the InAs channel.

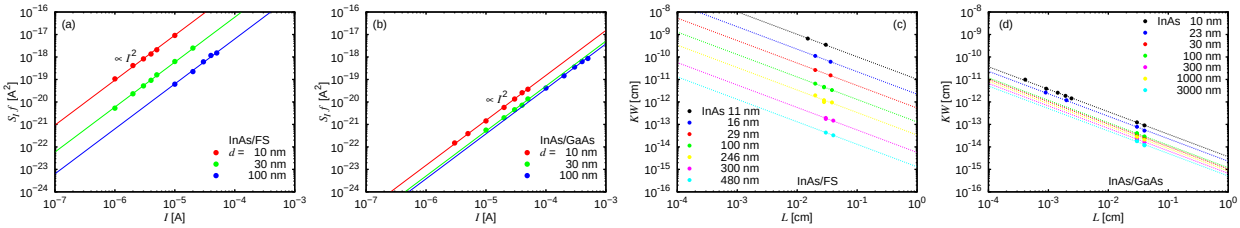

Figure 3: S_If as functions of I for (a) InAs/FS and (b) InAs/GaAs. The factor KW as functions of L for (c) InAs/FS and (d) InAs/GaAs.

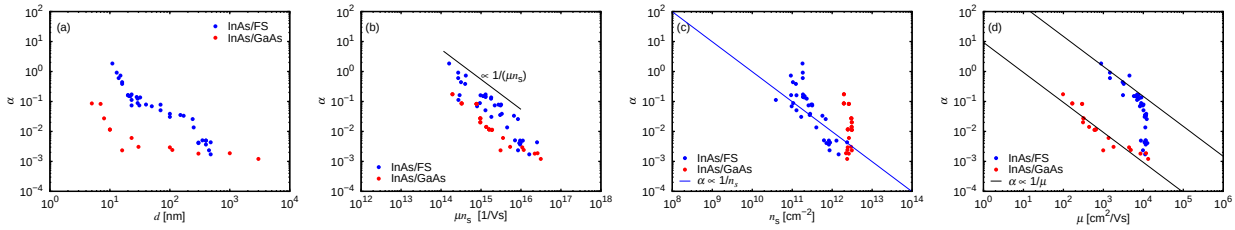

Figure 4: Hooge parameter α in InAs films as functions of (a) the InAs thickness d, (b) the product μn_s, (c) the sheet electron concentration n_s, and (d) the electron mobility μ.

Figure 4 shows α as functions of (a) d, (b) μn_s, (c) n_s, and (d) μ. The Hooge parameter is given by $\alpha = \dfrac{1}{\ln(f_h/f_\ell)}\left(\dfrac{(\delta\mu)^2}{\mu^2} + \dfrac{(\delta N)^2}{N}\right)$, where f_h and f_ℓ are the high and low limits of the $1/f$ behavior [8]. For InAs/FS with $d \gtrsim 20$ nm, where μ weakly changes as seen in Fig. 2(b), $\alpha \propto {n_s}^{-1}$ is observed and attributed to the carrier-number fluctuation $(\delta N)^2 \sim LWD_ik_BT$, where the interface state density $D_i \sim 10^{12}$ cm^{-2}eV^{-1} is obtained from the data, being consistent with the Coulomb-scattering mobility [5]. For InAs/FS with $d \lesssim 20$ nm and InAs/GaAs(001), where n_s weakly changes as seen in Fig. 2(b), $\alpha \propto \mu^{-1}$ is observed, which can be related to the mobility fluctuation due to constant fluctuations in the InAs thickness.

3 Low-frequency noise in AlGaN/GaN heterostructure

Figure 5(a) shows the product of the resistance R and the device width W as functions of the electrode spacing L for ungated 2T GaN devices, exhibiting a significant contribution of the contacts. The LFN spectra shown in Figs. 5(b)-(d) exhibit that S_I satisfies $S_I/I^2 \simeq K/f$, where K is a constant depending on device size.

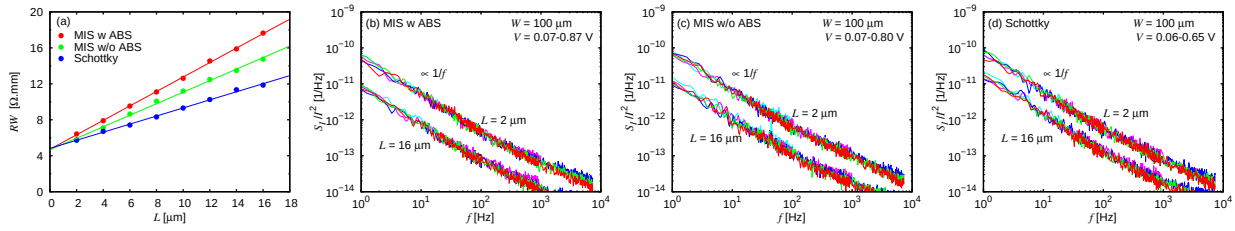

Figure 5: (a) The product of the resistance R and the device width W as functions of the electrode spacing L. S_I/I^2 as functions of f for GaN ungated 2T devices, (b) MIS w ABS, (c) MIS w/o ABS, and (d) Schottky devices.

Figures 6(a)-(c) show S_If as functions of I to determine K shown in Fig. 6(d). The ungated 2T GaN devices show $K \simeq$ constant for small L, indicating a significant contribution of the electrode contacts. Since the device resistance is the sum of the contact resistance and the ungated-channel resistance, we also obtained Eq. (1). Fitting data by Eq. (1), we obtained $K_cW \simeq 1.9 \times 10^{-12}$ cm for one contact, which is common for the MIS and Schottky devices because of the same Ohmic process, and a Hooge parameter of the ungated region

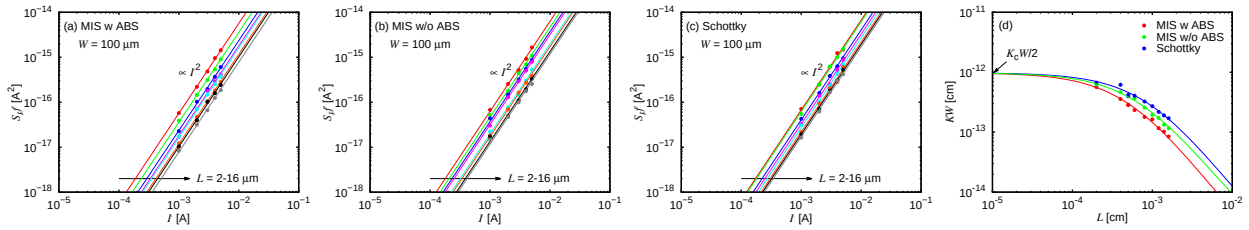

Figure 6: $S_I f$ as functions of I for GaN ungated 2T devices, (a) MIS w ABS, (b) MIS w/o ABS, and (c) Schottky devices. (d) The factor KW as functions of L for GaN ungated 2T devices.

$\alpha_{\rm ug} \simeq 2.2 \times 10^{-4}$ for the ungated 2T MIS devices with cleaning by ABS (w ABS), 4.1×10^{-4} for MIS devices w/o ABS, and 5.0×10^{-4} for Schottky devices. The smaller $\alpha_{\rm ug}$ in the MIS devices can be attributed to the lower electron mobility due to additional scattering mechanisms caused by the AlN insulator deposition, where the mobility fluctuation dominates $\alpha_{\rm ug}$ according to the Hooge theory [8].

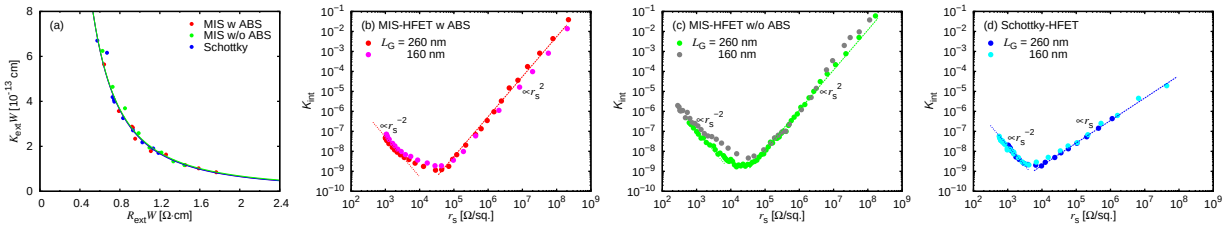

Figure 7: (a) $K_{\rm ext}W$ as functions of $R_{\rm ext}W$ for the ungated part of the GaN devices. The factor $K_{\rm int}$ as functions of the sheet resistance $r_{\rm s}$ of the gated region of GaN HFETs for (b) MIS w ABS, (c) MIS w/o ABS, and (d) Schottky devices.

The channel-current-dominated LFN in the linear regime of the GaN HFETs shows $S_{I_{\rm D}} \simeq K_{\rm HFET} {I_{\rm D}}^2/f$ with the drain current $I_{\rm D}$ and a constant factor $K_{\rm HFET}$ depending on the gate-source voltage $V_{\rm G}$. From the ungated-device characterization, LFN behavior in the intrinsic gated region was extracted for the HFETs. Since the on-resistance $R_{\rm on}$ given by the series connection of the intrinsic resistance $R_{\rm int} = r_{\rm s}L_{\rm G}/W$ with the sheet resistance $r_{\rm s}$ of the gated region and the gate length $L_{\rm G}$, and the extrinsic resistance $R_{\rm ext}$ of the ungated part,

$$K_{\rm HFET} = K_{\rm int}\frac{{R_{\rm int}}^2}{{R_{\rm on}}^2} + K_{\rm ext}\frac{{R_{\rm ext}}^2}{{R_{\rm on}}^2}, \tag{2}$$

where $K_{\rm int}$ is the factor for the intrinsic noise depending on $V_{\rm G}$, and $K_{\rm ext}$ is the factor for the extrinsic noise independent of $V_{\rm G}$. From the value of the $R_{\rm ext}$ obtained by DC characterization, we can evaluate $K_{\rm ext}$ of the ungated part using the relation given in Fig. 7(a), and consequently $K_{\rm int}$ by Eq. (2), as shown in Figs. 7(b)-(d). For the small $r_{\rm s}$ below the middle of 10^3 Ω/sq. range, $K_{\rm int} \propto {r_{\rm s}}^{-2}$ for both the MIS- and Schottky-HFETs. On the other hand, the MIS-HFETs for $r_{\rm s} \gtrsim 10^5$ Ω/sq. exhibit $K_{\rm int} \propto {r_{\rm s}}^2$, while the Schottky-HFETs for $r_{\rm s} \gtrsim 10^4$ Ω/sq. exhibit $K_{\rm int} \propto r_{\rm s}$. The factor $K_{\rm int}$ is given by $K_{\rm int} = \alpha/N = \alpha/n_{\rm s}L_{\rm G}W$, where $n_{\rm s}$ is the sheet electron concentration of the gated region. We obtained $n_{\rm s}$ by integration of the capacitance by measuring capacitors fabricated simultaneously with the HFETs. As a result, we obtain the Hooge parameter α as functions of $n_{\rm s}$, shown in Fig. 8 with the point of $\alpha_{\rm ug}$ for the ungated region.

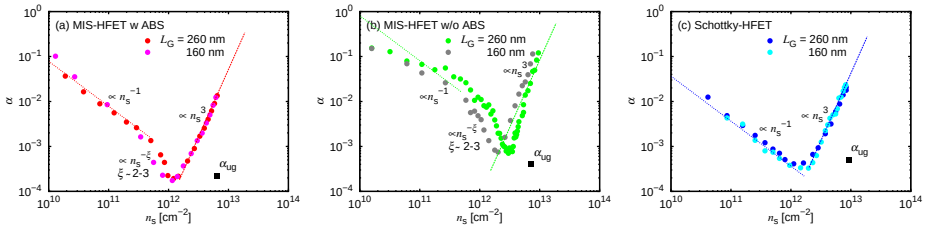

Figure 8: The Hooge parameter α as functions of the sheet electron concentration $n_{\rm s}$ of the gated region of GaN HFETs for (a) MIS w ABS, (b) MIS w/o ABS, and (c) Schottky devices. The point of $\alpha_{\rm ug}$ is for the ungated region.

For the MIS-HFETs with the small $n_{\rm s} \lesssim 5 \times 10^{11}$ cm^{-2}, $\alpha \propto {n_{\rm s}}^{-1}$, also observed for Schottky-HFETs with $n_{\rm s} \lesssim 10^{12}$ cm^{-2}, and is attributed to the carrier-number fluctuation due to electron traps with density

$D_0 \sim 10^{11}$ cm^{-2}eV^{-1} in the AlGaN. On the other hand, for 5×10^{11} cm^{-2} $\lesssim n_s \lesssim 1 \times 10^{12}$ cm^{-2}, the MIS-HFETs show $\alpha \propto {n_s}^{-\xi}$ with $\xi \sim$ 2-3, which is not observed for Schottky-HFETs, and tentatively attributed to the mobility fluctuation specific for the MIS-HFETs. Moreover, $\alpha \propto {n_s}^3$ for both MIS- and Schottky-HFETs with $n_s \gtrsim 2 \times 10^{12}$ cm^{-2}, can be attributed to the fluctuation in the intrinsic gate voltage, which is enhanced for large gate voltage and n_s by the fluctuation of the voltage across the extrinsic source resistance.

4 Conclusion

LFN in narrow- and wide-gap III-V compound semiconductors were systematically investigated for InAs (narrow-gap) and GaN (wide-gap) devices. We clarified detailed behaviors of the Hooge parameter depending on the devices.

References

[1] M. Tacano, M. Ando, I. Shibasaki, S. Hashiguchi, J. Sikula, and T. Matsui, Microelectron. Reliab. **40**, 1921 (2000).

[2] M. E. Levinshtein, F. Pascal, S. Contreras, W. Knap, S. L. Rumyantsev, R. Gaska, J. W. Yang, and M. Shur, Appl. Phys. Lett. **72**, 3053 (1998).

[3] N. Pala, R. Gaska, S. Rumyantsev, M. Shur, M. A. Khan, X. Hu, G. Simin, and J. Yang, Electron. Lett. **36**, 268 (2000).

[4] H. Takita, N. Hashimoto, C. T. Nguyen, M. Kudo, M. Akabori, and T. Suzuki, Appl. Phys. Lett. **97**, 012102 (2010).

[5] C. T. Nguyen, H.-A. Shih, M. Akabori, and T. Suzuki, Appl. Phys. Lett. **100**, 012102 (2012).

[6] H.-A. Shih, M. Kudo, M. Akabori, and T. Suzuki, Jpn. J. Appl. Phys. **51**, 02BF01 (2012).

[7] H.-A. Shih, M. Kudo, and T. Suzuki, Appl. Phys. Lett. **101**, 043501 (2012).

[8] F. N. Hooge, T. G. M. Kleinpenning, and L. K. J. Vandamme, Rep. Prog. Phys. **44**, 479 (1981).

Table of contents

List of publications

1. S. P. Le, M. Akabori and T. Suzuki: "Electron mobility anisotropy in InAs/GaAs(001)", The seventeenth International Conference on Molecular Beam Epitaxy, Nara, Japan, September 23-28 (2012).
2. S. P. Le, T. Q. Nguyen, H.-A. Shih, M. Kudo and T. Suzuki: "Low-frequency noise of intrinsic gated region in AlN/AlGaN/GaN metal-insulator-semiconductor heterojunction field-effect transistors", International Conference on Solid State Devices and Materials, Tsukuba, Japan, September 8-11 (2014).
3. S. P. Le, T. Q. Nguyen, H.-A. Shih, M. Kudo and T. Suzuki: "Low-frequency noise in AlN/AlGaN/GaN metal-insulator-semiconductor devices: a comparison with Schottky devices", Journal of Applied Physics **116** (2014) 054510.

Keywords

III-V compound semiconductors, InAs, AlGaN/GaN, low-frequency noise, Hooge parameter.

論文審査の結果の要旨

本論文では、異種材料間の界面が重要な役割を果たしているナローギャップおよびワイドギャップ III-V 族化合物半導体デバイスについて、低周波ノイズを調べた結果が示されている。

エレクトロニクスの機能的多様化に向け、ナローギャップおよびワイドギャップ化合物半導体デバイスの重要性は高い。化合物半導体デバイスの異種材料融合技術は、多く機能の実現を可能にすることが期待されるが、同時に、異種材料間界面を有するデバイスにおいては、界面が低周波ノイズに与える影響が懸念される。デバイスの低周波ノイズは、高周波発振器応用における位相ノイズなどの問題を引き起こすため、その理解と制御は応用上重要である。そこで、本研究では、自作の回路を含む低周波(1 Hz - 10 kHz)ノイズ計測システムを構築し、ナローギャップ化合物半導体 InAs を用いたデバイスと、ワイドギャップ化合物半導体 GaN を用いたデバイスについて、低周波ノイズ計測と、計測結果の解析が行われた。

まず、所属研究室独自の手法であるエピタキシャルリフトオフ-貼付によって作製されたフレキシブル基板上 InAs 薄膜ホールバーデバイスについて、その低周波ノイズの計測が初めて系統的に行われた。このデバイスにおける電子移動度は、GaAs(001)基板上 InAs 薄膜ホールバーデバイスより高く、優れた DC 特性を示すが、低周波ノイズは寧ろ大きく、劣っていることが明らかになった。これにより、優れた DC 特性を示すデバイスであっても、低周波ノイズに課題を有する場合があることが浮き彫りになった。解析の結果、この大きい低周波ノイズは、貼付によって形成された異種材料界面における界面準位での電子捕獲・放出による電子数揺らぎと、移動度揺らぎの双方によってもたらされていることが示された。

さらに、スパッタリング堆積によるアモルファス AlN ゲート絶縁膜を用いた AlN/AlGaN/GaN 金属-絶縁体-半導体(MIS)デバイスについて、その低周波ノイズの計測が初めて系統的に行われた。その結果、デバイス内の真性部分と寄生部分の低周波ノイズに対する寄与が明らかとなった。また、ショットキーゲートを用いたデバイスでは見られない、MIS ゲートを用いたデバイスに特有な低周波ノイズの挙動が見出された。さらに、AlN-AlGaN 界面の低周波ノイズへの影響が非常に小さいことが示された。これは、界面準位での電子捕獲・放出が非常に長い時定数を有するためであると考えられ、上記のナローギャップデバイスの場合と対照的である。

以上のように、本論文では、化合物半導体デバイスの低周波ノイズについて、新規かつ有用な結果が得られており、学術的および産業的な価値が大きい。よって博士(マテリアルサイエンス)の学位論文として充分価値あるものと認めた。